Eur Biophys J (2006) 35:621–632
DOI 10.1007/s00249-006-0068-4

ARTICLE

Optimizing crystal volume for neutron diffraction: D-xylose isomerase

Edward H. Snell · Mark J. van der Woerd · Michael Damon · Russell A. Judge · Dean A. A. Myles · Flora Meilleur

Received: 15 February 2006 / Revised: 27 March 2006 / Accepted: 4 April 2006 / Published online: 25 May 2006

Abstract Neutron diffraction is uniquely sensitive to hydrogen positions and protonation state. In that context structural information from neutron data is complementary to that provided through X-ray diffraction. However, there are practical obstacles to overcome in fully exploiting the potential of neutron diffraction, i.e. low flux and weak scattering. Several approaches are available to overcome these obstacles and we have investigated the simplest: increasing the diffracting volume of the crystals. Volume is a quantifiable metric that is well suited for experimental design and optimization techniques. By using response surface methods we have optimized the xylose isomerase crystal volume, enabling neutron diffraction while we determined the crystallization parameters with a minimum of experiments. Our results suggest a systematic means of enabling neutron diffraction studies for a larger number of samples that require information on hydrogen position and/or protonation state.

E. H. Snell (✉)
Hauptman-Woodward Medical Research Institute,
700 Ellicott Street, Buffalo, NY 14203, USA
e-mail: esnell@hwi.buffalo.edu

M. J. van der Woerd · M. Damon
BAE Systems, 308 Voyager Way,
Huntsville, AL 35806, USA

R. A. Judge
Abbott Laboratories, Abbott Park, IL 60064 , USA

D. A. A. Myles
Oak Ridge National Laboratory, P.O. Box 2008,
Oak Ridge, TN 37831, USA

F. Meilleur
Institut Laue Langevin, BP 156, 38042 Grenoble, France

Introduction

Neutron diffraction

X-ray structural crystallography is a powerful technique to visualize the machinery of life on a molecular scale. However, hydrogen atoms are not usually seen because X-ray scattering from hydrogen atoms is weak compared to other atoms. Knowledge of the location of hydrogen atoms and water molecules is often necessary to completely understand the reaction mechanisms, pathways and structure–function relationships. Neutron crystallography offers an approach to visualize these atoms. The scattering amplitudes for neutrons vary from element to element in a non-systematic way. Deuterium atoms have a large neutron scattering amplitude, similar to other atoms typically found in macromolecules. Neutron diffraction data at ~2 Å resolution can unambiguously define hydrogen positions.

Structures derived from neutron diffraction data are not common due to practical difficulties which limit the use of the technique. Neutron sources have relatively low flux compared to synchrotron X-ray beam lines and the scattering of neutrons is weak. The neutron flux and diffraction signal have to be maximized and the noise minimized to enable optimum experimental results. Table 1 summarizes several complementary

Table 1 Summary of different approaches to improve reflection intensity from neutron diffraction divided into increasing neutrons, improving the instrument, reducing the noise or increasing the sample volume

Solution	Relative cost	Time	Success
More neutrons			
Increase source intensity	Very expensive	Long term	Certain
Reduce distance to source	Expensive	Medium term	Certain
Increase exposure time	Inexpensive but reduces experimental throughput	Short term	Certain
Improved detection/optics			
New and improved detector technology	Expensive	Medium term	Good
Focusing optics	Moderately expensive	Medium term	Good
Improve signal-to-noise			
Deuteration	Relatively inexpensive	Short term	Good
Diffracting volume			
Grow larger crystals	Inexpensive	Short term	Good

All the approaches are complementary and cumulative. They are assessed by the relative cost, time and success of implementation

pathways to achieve this goal with a qualitative estimate of the relative cost, time and chance of success. Certain solutions, i.e. increasing the neutron flux or improving the detection of the signal, are beyond the resources of an individual user and are being addressed at the facility level e.g. in the construction of dedicated instruments on new neutron sources such as the Spallation Neutron Source (SNS), USA, and the Japan Proton Accelerator Complex (J-PARC). Other techniques, for example improving the signal-to-noise ratio by perdeuteration (replacing hydrogen with deuterium atoms) may be routinely attempted (Meilleur et al. 2005) and can dramatically decrease the volume of sample needed for successful data collection (Hazemann et al. 2005; Shu et al. 2000).

The diffraction intensity, I, can be expressed as (Niimura 1999);

$$I = \frac{I_0 F^2 V A}{v_0^2} \quad (1)$$

where I_0 is the incident intensity, F the structure factor, V the illuminated volume of the crystal, A the detector area subtended by the crystal and v_0 the unit cell volume. This equation shows that the measured signal is directly proportional to the crystal volume V. Unlike the X-ray case, absorption by the sample is minimal for neutron diffraction and therefore volume optimization directly benefits the diffraction data signal.

Optimization of crystal growth

Crystal growth depends on multiple parameters, such as temperature, concentration of components in the experiment and the crystallization method used. Figure 1 illustrates a simplified phase diagram for two parameters, the macromolecule concentration and the precipitant concentration (Chayen 1998). Different crystallization techniques are available: vapor diffusion, dialysis, free interface diffusion and batch crystallization. The pathways of these methods are illustrated in the figure. For the purpose of crystal size optimization it is desirable to use the smallest amount of sample possible and to make the technique readily scalable for use with a large amount of sample to produce the crystals for diffraction experiments. Vapor diffusion and, to some extent, dialysis techniques are problematic for systematic study because multiple parameters are changing over the course of the experiment and it is therefore difficult to assess the influence of a single parameter on the experimental result. The conditions during the experiment depend on, among other parameters, the pathway in the phase diagram, the volume of the experiment, the surface areas involved and transport physics. Free interface crystallization is now commercially available for screening in small volumes, but the production of crystals large enough for diffraction experiments remains a challenge. Fortunately, there is another technique, the batch method. In this method, the crystallization solutions are premixed and the experiment can easily be scaled up by making use of large volumes and more material. It is conceptually also the simplest technique and by definition the initial conditions are well characterized. For our optimization experiments this has been the method of choice.

The interrelationship between variables means that simply exploring crystallization space one variable at a time is inefficient and fails to provide information on interactions. The optimum approach to understand and predict the effect of several factors with the minimum number of experiments is to conduct a factorial experiment. This is an experimental strategy in which factors are varied together instead of individually.

The use of factorial design in crystallography has been pioneered by Carter and Carter (1979) and used successfully both to understand and optimize crystallization conditions (Burke et al. 2001; Carter 1994).

Good experimental design requires a clear statement of the problem, a choice of factors, levels and ranges, the selection of response variables, choice of experimental design, good experimental technique and a statistical analysis of the results. Our problem is clearly defined, i.e. how to grow crystals with as large an illuminated volume as possible. This is also easily measured, as crystal dimensions and their volume are quantitative metrics. For the purposes of neutron diffraction we are fortunate in that the crystallization conditions have usually been developed and optimized for X-ray data collection. We therefore have a good idea of the choice of factors, levels and ranges that result in crystals and can also make an informed decision on the choice of response variables.

From previous experience and phase diagrams similar to Fig. 1 we can predict that the interaction between variables will be non-linear so we can expect to use a second-order model which guides our choice of experimental design. This is the simplest model that provides interactive terms. We do not know where the optimum condition lies so a central composite design allows us to sample the experimental space where equal precision of estimate is achieved in all directions. The central composite design for two variables is illustrated in Fig. 2. It has nine individual points consisting of the center, four points on a circle looking at variable interactions and four outlying points at the maximum and minimum of the variable range being studied.

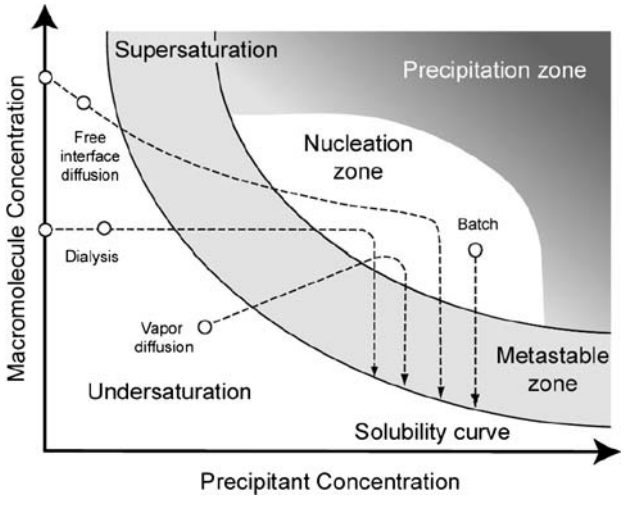

Fig. 1 A schematic illustration of the macromolecular crystallization phase diagram based on two of the most commonly varied parameters, macromolecule and precipitant concentrations. The four main crystallization methods are highlighted showing that, in order to produce crystals, all the systems need to reach the same destination, the nucleation zone. In the case of dialysis and free interface diffusion (also called liquid/liquid diffusion) two alternative starting points are shown since the undersaturated macromolecular solution can contain solely the macromolecule or alternatively, the macromolecule with a low concentration of the precipitating agent (adapted from Chayen 1998)

Deuteration

Hydrogen atoms produce significant background noise in neutron diffraction due to their large incoherent scattering contribution. Perdeuteration is a technique whereby all hydrogen atoms are replaced with deuterium. When using this technique the background noise is significantly reduced. However, there are several levels of deuteration attainable that are experimentally increasingly demanding; the growth or soaking of the crystal in solutions made up from D_2O provides partial deuteration; using deuterated reagents in addition will improve the deuteration level and finally; the synthesis of a fully deuterated macromolecule. Exchangeable hydrogen only accounts for about 25% of the total hydrogen atoms in a crystal (Shu et al. 2000) so the preferred method is perdeuteration however it is not always possible or practical to reach complete deuteration.

H_2O and D_2O have different biophysical properties. For example, the maximum density of D_2O occurs at 11.2°C compared with 4.0°C for H_2O, a shift of 7.2°C. Interestingly, in the few cases studied, lysozyme and aprotinin, a reduction in solubility is reported for D_2O solutions (Broutin et al. 1995; Budayova-Spano et al. 2000; Liu and Sano 1998a, b). When the temperature of the D_2O solution is raised by 7.2°C, the protein solubility matches the solubility for H_2O-based solutions (Budayova-Spano et al. 2000; Gripon et al. 1997a, b). Deuteration also has biochemical consequences, the

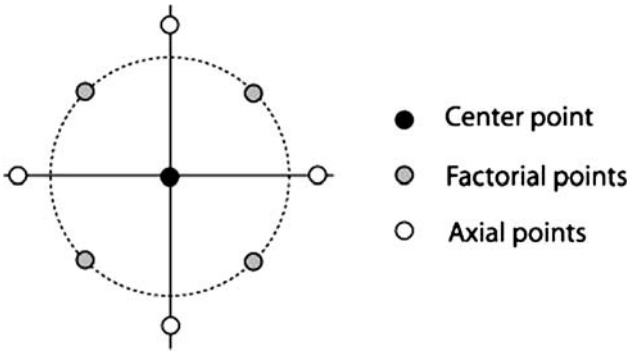

Fig. 2 Schematic illustrating the data points in a two-dimensional central composite design. This can be expanded to three or more dimensions but is kept at two for clarity in describing the method

pD of a solution in D_2O is 0.4 above the measured pH of the solution (Glasoe and Long 1960).

In this paper we report the use of experimental design methods to optimize the growth of large xylose isomerase crystals for neutron diffraction studies. We look at the number of experiments needed, the choice of variables and the influence that using D_2O in place of water has on the optimization.

Experimental

Protein sample

Xylose isomerase, molecular weight of 172 kDa (a homotetramer with 43 kDa subunits) is an enzyme used industrially to catalyze the reversible isomerisation between glucose and fructose. The conversion of D-glucose to D-fructose consists of a hydrogen transfer between carbon C_1 and C_2 of the substrate. The mechanistic interest in D-xylose isomerase originates from the fact that it appears to catalyze an isomerisation reaction not by proton-transfer mechanism but by a hydride shift, promoted by a bridged bimetallic center (Asboth and Naray-Szabo 2000; Carrell et al. 1989; Farber et al. 1989; Fenn et al. 2004).

Xylose isomerase from *Streptomyces rubiginosus* was obtained from Genencor International as a concentrated brown liquid and purified by size exclusion chromatography over Sephacryl S200 resin (GE Biosciences). The fractions were pooled and dialyzed against distilled water at room temperature. The final dialysis was against 0.05 g/l magnesium sulfate. The purity of the glucose isomerase was verified with Capillary Electrophoresis.

Xylose isomerase solubility was determined at pH 7.7 and 22°C, over an ammonium sulfate concentration range of 10–18% (w/v). No buffer was used; the pH was adjusted by adding dilute ammonia or sulfuric acid. Solubility was determined by batch crystallization and by dissolution of crystals grown by the batch method, using solution volumes of 200 µl contained in Eppendorf tubes. Protein concentration in solution was measured over time by UV absorbance (using an absorbance value of $A(1\%,\ 1\ \text{cm}) = 10.9$). Protein solubility was determined at equilibrium conditions when the protein concentration was observed to reach a steady concentration (after approximately 5 weeks). The reported solubility data are the average value determined by crystallization and dissolution results. Experiments were done in duplicate (i.e., two crystallization and dissolution pairs). The fit to the solubility data, Fig. 3, is given by,

$$\log_{10}(S) = 1.62 - 0.054A \quad (2)$$

Where S is the xylose isomerase solubility in mg/ml and A is the ammonium sulfate concentration in %(w/v). The fit gave an r^2 value of 0.94.

Experimental design

Supersaturation is defined as $\ln(c/s)$ where c is the bulk solution concentration and s is the solubility concentration. Supersaturation and therefore solubility are key parameters in many theoretical models of crystal growth but it is not typical to have this information for a macromolecule of interest. In our experimental design we have examined two approaches, designing the experiment with the use of solubility data and the more typical case of optimization without these data.

Experimental design using solubility data

A central composite design, as shown in Fig. 4a was set up over a range of ammonium sulfate concentration of 10–18% (w/v) and a corresponding supersaturation of 1.8–2.4. Expressed in protein concentration, for comparison with the design setup without the knowledge of solubility Fig. 4b, these conditions range from 44 to 80 mg/ml xylose isomerase (using 14% ammonium sulfate as precipitant). A xylose isomerase stock solution at a concentration of 135 mg/ml was used for the crystallization experiments. It was centrifuged at 16,000*g* for 10 min before use. Experiments were performed with four replicates for each condition with eight central points, giving a total of 40 experiments. The batch crystallization experiments were set

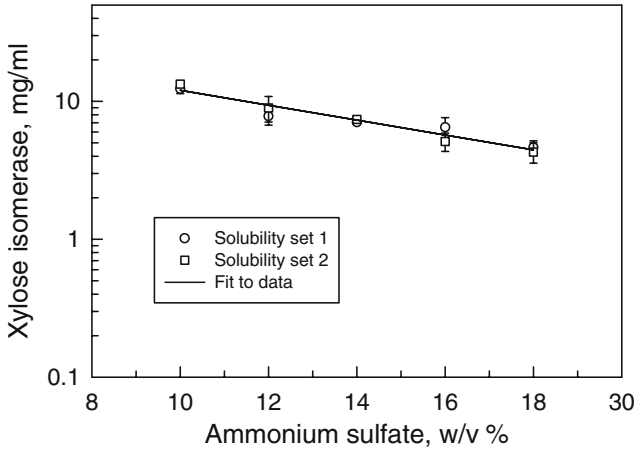

Fig. 3 Xylose isomerase solubility in ammonium sulfate solutions at pH 7.7 and 22°C

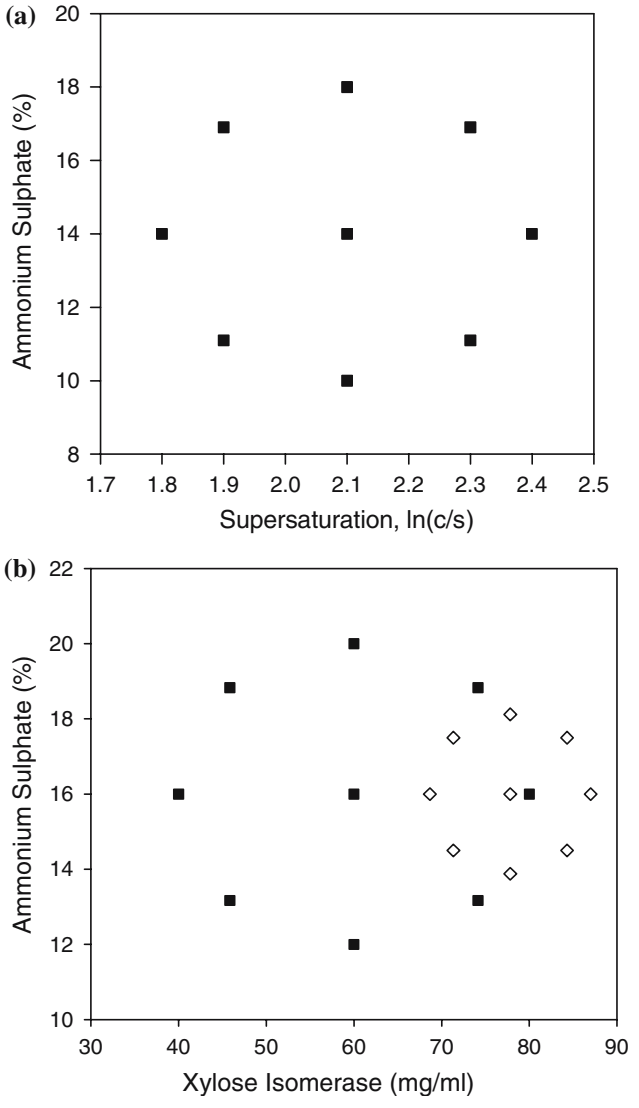

Fig. 4 Two-dimensional experimental design for optimization **a** with and **b** without solubility data for xylose isomerase. The *open circles* in (**b**) illustrate the second round of optimization based on the first round results

up in sitting drop vapor diffusion plates using 25 µl drops. The drops were mixed by pipette after dispensing the solution components to the well. The outer reservoir was filled with 1 ml of the same ammonium sulfate concentration as the drop to maintain the precipitant concentration in the drop over time. The plates were covered with clear tape and incubated at 22°C. After 7 days, each crystallization well was imaged and the crystal number and size were recorded. Crystal size is given as the area equivalent diameter (i.e., the visible crystal area was measured and the size is given as the diameter of a circle of the same area).

The model upon which the central composite design is based is given by;

$$Y = b_0 + b_1X_1 + b_2X_2 + b_{12}X_1X_2 + b_{11}X_1^2 + b_{22}X_2^2 \quad (3)$$

where Y is the observed response, b_0 is a coefficient, b_1 is the coefficient for the main effect of precipitant concentration (X_1), b_2 is the coefficient for the main effect of supersaturation (X_2), b_{12} is the coefficient for the interactive effect of precipitant concentration and supersaturation (X_1X_2), b_{11} is the coefficient for the curvature for precipitant concentration (X_1^2) and b_{22} is the coefficient for curvature of supersaturation (X_2^2). The measured response in this case was crystal number and crystal size.

Experimental design without solubility data

A central composite design was set up as shown in Fig. 4(ii). For the purposes of this study 72 experiments were set up, 8 individual experiments at each of the 9 conditions. The number eight was chosen to evaluate how many experiments were needed to provide a reliable prediction. The experiments were carried out in 72-well Nunc plates using 4 ml total of precipitant and protein solution and the drops were sealed by adding paraffin oil on top of the drops.

To study the effects of temperature, crystals were grown in incubators at 18, 22, and 26°C, and observed over time using a microscope. Once growth had slowed to the point where there was no measurable difference between subsequent observations the resulting crystals were measured and counted. The data were fitted to a response surface described by Eq. 3. Guided by the predicted results from the response surface, a second iteration took place using a narrower range of conditions, including an additional temperature point, 14°C, and a central condition shifted away from the center used in the first iteration, see Fig. 4b.

Deuteration considerations

Deuteration should always be attempted, at a minimum by soaking the crystal in mother liquor containing D_2O because even partial deuteration will improve the signal-to-noise ratio in neutron diffraction experiments. We repeated the above experiments at 22°C with a slightly reduced sampling range, using D_2O solutions at the same pH, and at a value of pH 0.4 units above that value to look at the effect of replacement of H_2O with D_2O on the optimization. As a potential

alternative, we also examined the effect of growing crystals in the non-deuterated solutions at pH 0.4 units below the optimum for H_2O.

Results

Results using solubility data

In the analysis of the results (number and size) a multi-linear regression was performed to determine the value and significance of the coefficients in Eq. 3. For the number of crystals generated the model is

$$\text{number} = 3.28 - 1.13X_1 + 0.62X_2 - 0.28X_1X_2 - 0.20X_1^2 + 0.13X_2^2 \quad (4)$$

where, X_1 represents precipitant concentration and X_2 supersaturation, i.e. ln(concentration/solubility). A regression analysis of the data (Design-Expert by Stat-Ease Inc., Minneapolis, MN, USA) shows that the

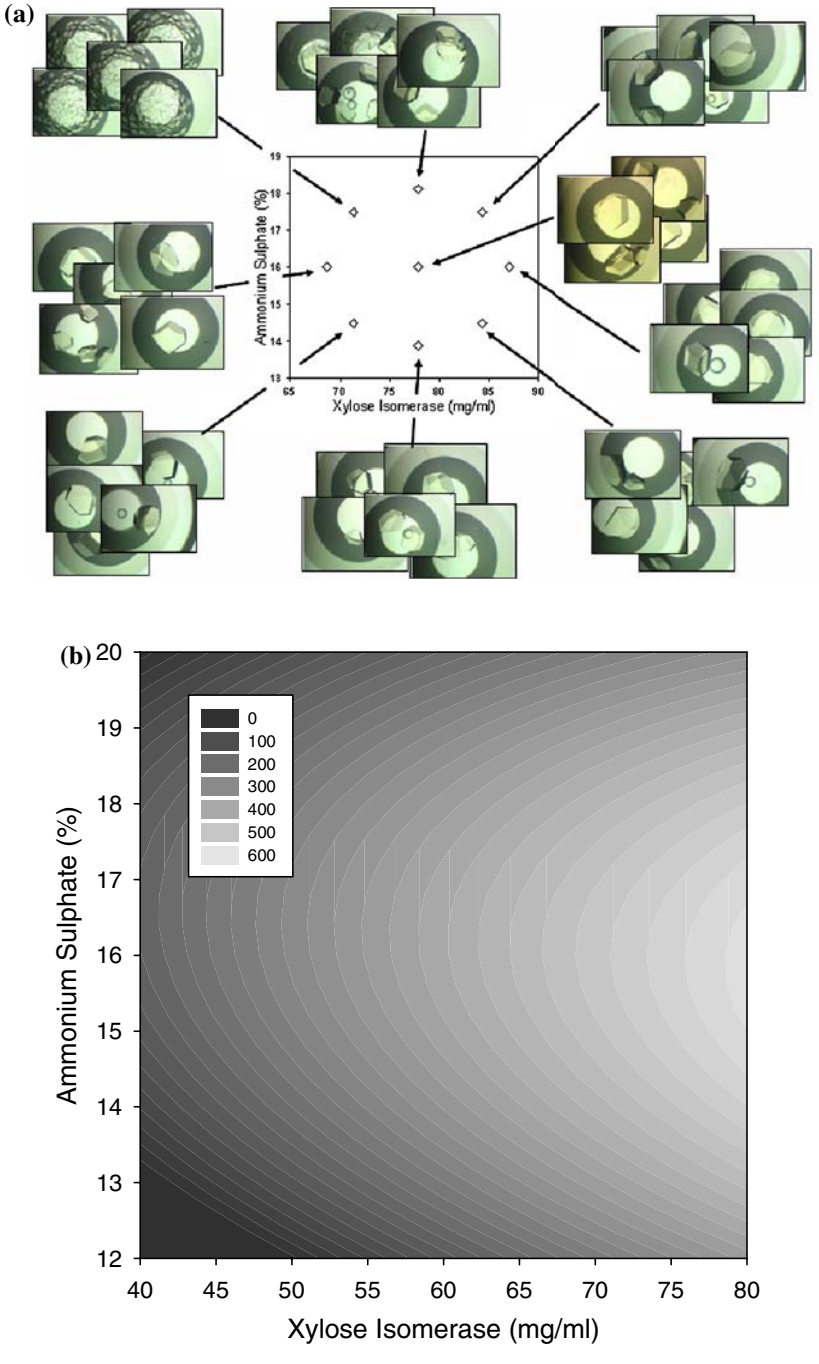

Fig. 5 **a** Crystals resulting from the first iteration based on screening protein and precipitant concentration and **b** the resulting response surface

main effect of precipitant concentration (X_1) is significant ($P < 0.01$) while the main effect of supersaturation (X_2) is just below the threshold to be considered statistically significant ($P > 0.05$) for the experimental outcome. The contributions of the interaction (X_1X_2) and quadratic terms (X_1^2, X_2^2) were found not to be statistically significant. Expressed in crystal growth language, the analysis shows that the number of crystals decreases with increasing precipitant concentration.

The model for crystal size is given by Eq. 5,

$$\text{size} = 949 - 38X_1 + 201X_2 + 79X_1X_2 + 160X_1^2 + 54X_2^2 \quad (5)$$

where the crystal size is expressed in μm, X_1 represents precipitant concentration and X_2 supersaturation. In this case the main effect of supersaturation is significant ($P < 0.001$) and the quadratic effect of precipitant concentration is significant ($P < 0.05$). The other terms were not statistically significant. The response curve shows that crystal size is primarily increased by increasing supersaturation. The curvature of the response surface due to precipitant concentration indicates that the largest crystals are obtained at high supersaturation and either low or high precipitant concentration. Crystal number increases at low precipitant concentrations (Eq. 4). High supersaturation and low precipitant concentration therefore produce many large crystals in the crystallization well, which inter-grow. Large individual crystals are obtained in the region of high supersaturation and high precipitant concentration.

Results without solubility data

A sample of crystals resulting from the first iteration is shown in Fig. 5a along with the conditions producing them. In this case the fit to the model for size, with X_1 and defined as above and X_2 as protein concentration in mg/ml, is given by;

$$\text{size} = -4,904 + 27X_1 + 520X_2 - 0.6X_1X_2 - 0.1X_1^2 - 15X_2^2 \quad (6)$$

and shown as a response surface in Fig. 5(ii). It can be clearly seen that the precipitant concentration is well optimized but based on the established response surface we can predict that an increase in protein concentration will further increase crystal size.

The second optimization was carried out with conditions shown in Fig. 4b. The fit to size at 22°C is given by

$$\text{size} = -14,277 + 37X_1 + 1,617X_2 + 11X_1X_2 - X_1^2 - 78X_2^2 \quad (7)$$

and a sample of crystals and response surface are shown in Fig. 6.

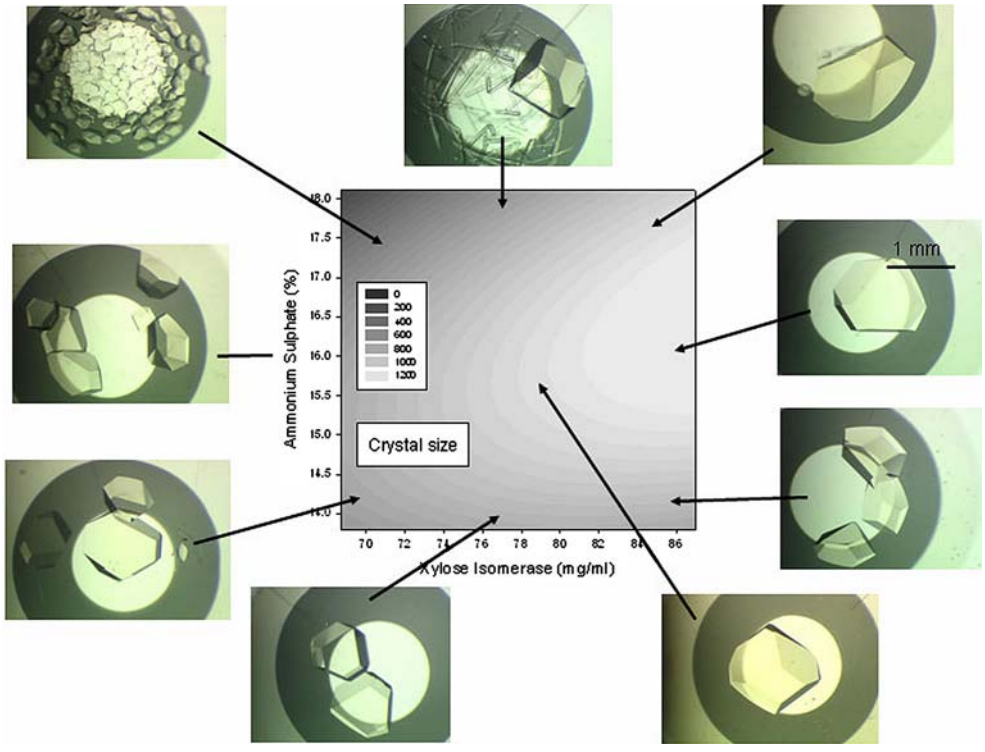

Fig. 6 Images of crystal number and size superimposed on the response surface given by Eq. 6

The equation can be extrapolated to a wider range of conditions to suggest which conditions will maximize volume than scaling up the volume with those conditions to achieve the largest crystal, see Fig. 7. A significant part of the response surface is outside the experimental sampling region and this reduces the reliability of the prediction. However, it does graphically illustrate the general direction to take to optimize the crystal size.

Temperature effects on crystal size

Table 2 lists the parameters in Eq. 3 for the initial size optimization experiment and for the second experiment, optimizing at temperatures of 14, 18, 22 and 26°C. With the temperature data and the response surfaces for precipitant and protein concentration we can predict the optimal conditions to grow the largest crystals, shown in Fig. 8. In this case the largest crystals are grown in a batch experiment at 18°C with 95 mg/ml xylose isomerase and 16.9% ammonium sulfate. A graphical analysis of the optimal growth conditions and how the parameters depend on temperature are shown in Fig. 9.

Table 2 Description of the crystal size response surfaces at various temperatures for the initial experiment and the second iteration

Temperature (°C)	b_0	b_1	b_2	b_{12}	b_{11}	b_{22}
Initial						
18	–5,024.4	29.0	523.5	–0.6	–0.1	–15.1
22	–4,904.6	26.9	520.4	–0.6	–0.1	–15.1
26	–4,810.1	21.7	522.8	–0.6	–0.1	–15.1
Second						
14	–12,654.0	34.1	1,537.4	10.7	–1.1	–77.7
18	–14,025.3	35.3	1,614.5	10.7	–1.1	–77.7
22	–14,277.1	36.6	1,617.6	10.7	–1.1	–77.7
26	–14,317.3	28.5	1,637.4	10.7	–1.1	–77.7

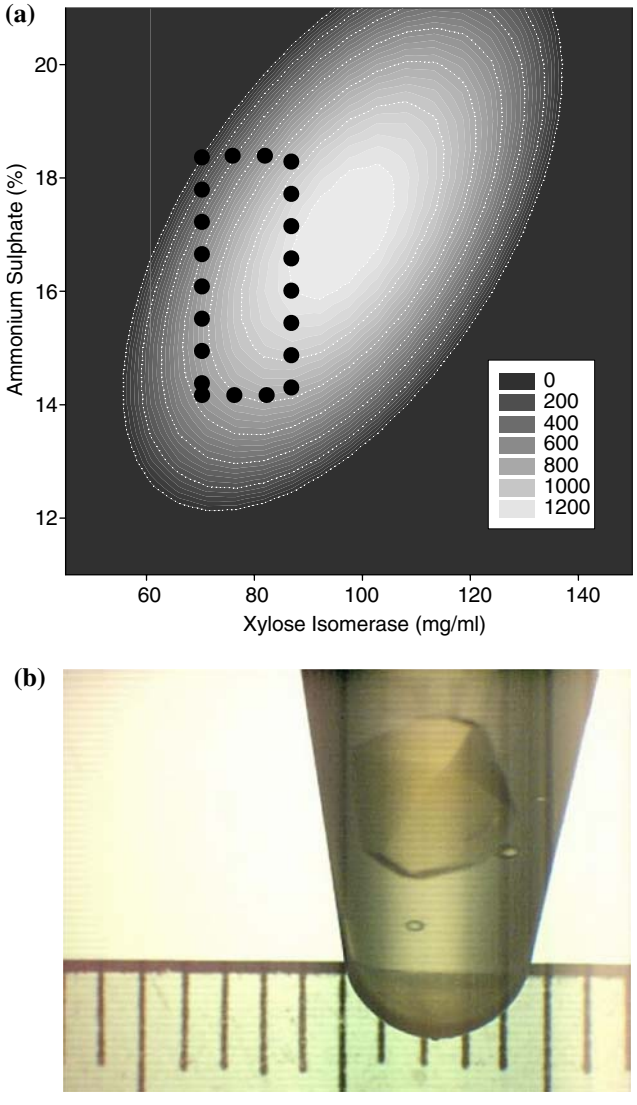

Fig. 7 **a** Predicted response surface, the *dotted area* is approximately equivalent to the area in Fig. 6, which was experimentally determined. **b** A typical optimized xylose isomerase crystal grown in a 1.5 ml Eppendorf tube—note in this case the crystal was grown in D_2O solution for neutron experimentation. Each small division on the scale is 1 mm

Statistical analysis

The statistical analysis was performed by Design-Expert and the outcome is shown in Table 3. The properties listed in this table are defined as follows. The model significance (F value) is the ratio of the model sum of squares to the residual sum of squares. A large number indicates that variance is being explained by the model, a smaller number indicates that variation is due to the noise in the data. For each case here the significance is high, with a 0.01% chance that the variation predicted by the model is due to noise. The lack of fit is the portion of the residual sum of squares due to the model not fitting the data. If the lack of fit is high, describing variation between replicated data points, then the model is not a perfect description of the process. However, in this case it is adequate for our purposes. The prediction power is a measure of the range in predicted response in relation to its associated error, in other words a signal-to-noise ratio, values over four are regarded as adequate. The adjusted R^2 is a measure of the amount of variation about the mean explained by the model adjusted for the number of terms. It is at a maximum of 100% when the model predicts 100% of the data. The predicted R^2 is a measure of the amount of variation in new data explained by the model. The adjusted and predicted

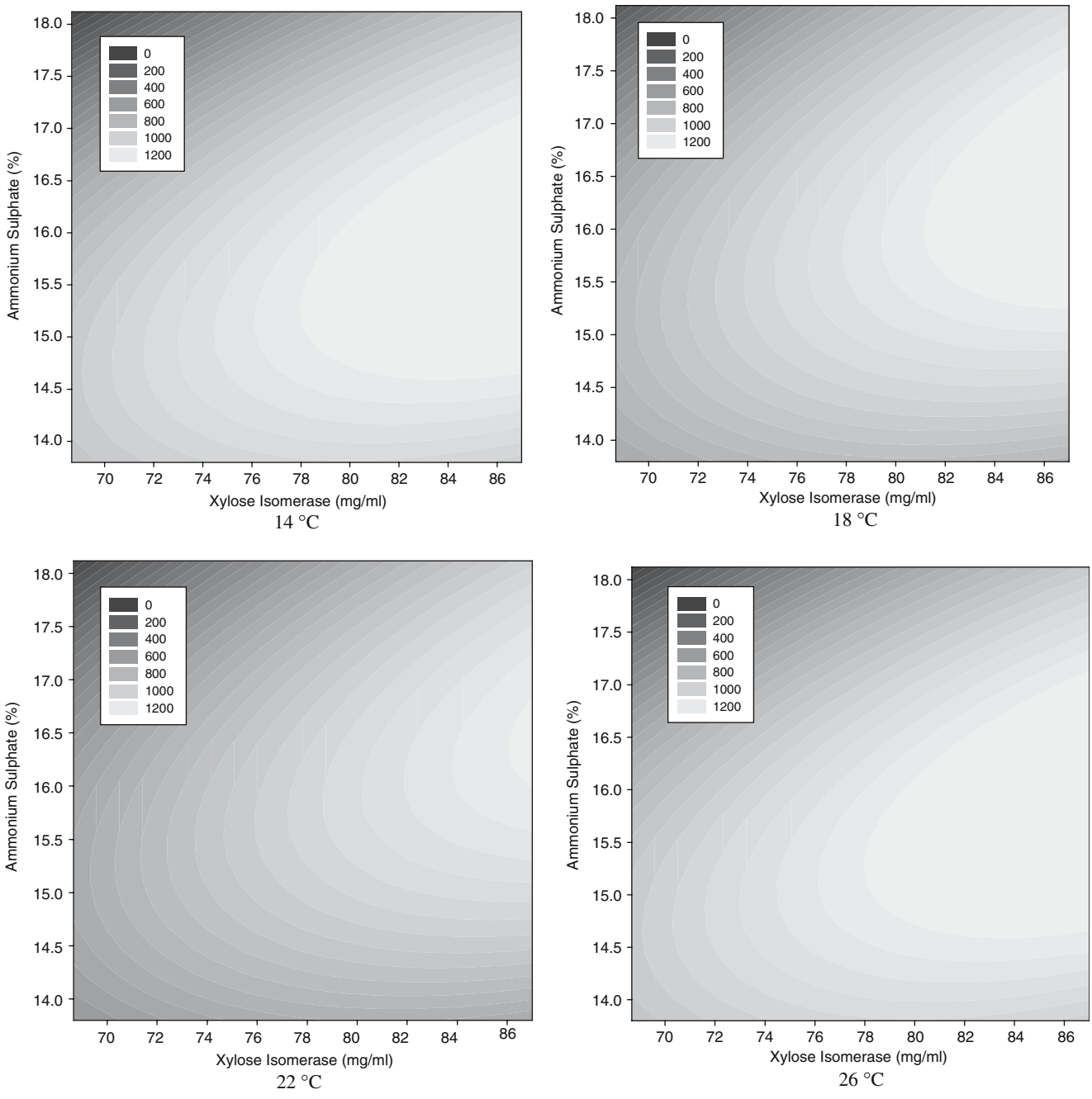

Fig. 8 Plot of a quadratic function of crystal size fitted as a function of precipitant and protein concentration at four separate temperatures. The area shown is the experimentally sampled area

R^2 should be within 0.2 of each other, greater differences than 0.2 indicate a problem with the data or the model.

Effect of deuteration

Table 4 illustrates the optimum conditions for crystal growth at 22°C for D_2O-based solutions at pH 7.3 and 7.7 (equivalent to pD 7.7 and 8.1, respectively) and H_2O-based solutions at pH 7.7 and 8.1 predicted on a course screen. It is clear that the conditions vary widely and simply changing pH of solution by 0.4 units to reflect the difference in measured pH between H_2O and D_2O solutions (Glasoe and Long 1960) does not produce improved conditions, in fact it seems to result in a decrease in the size obtained.

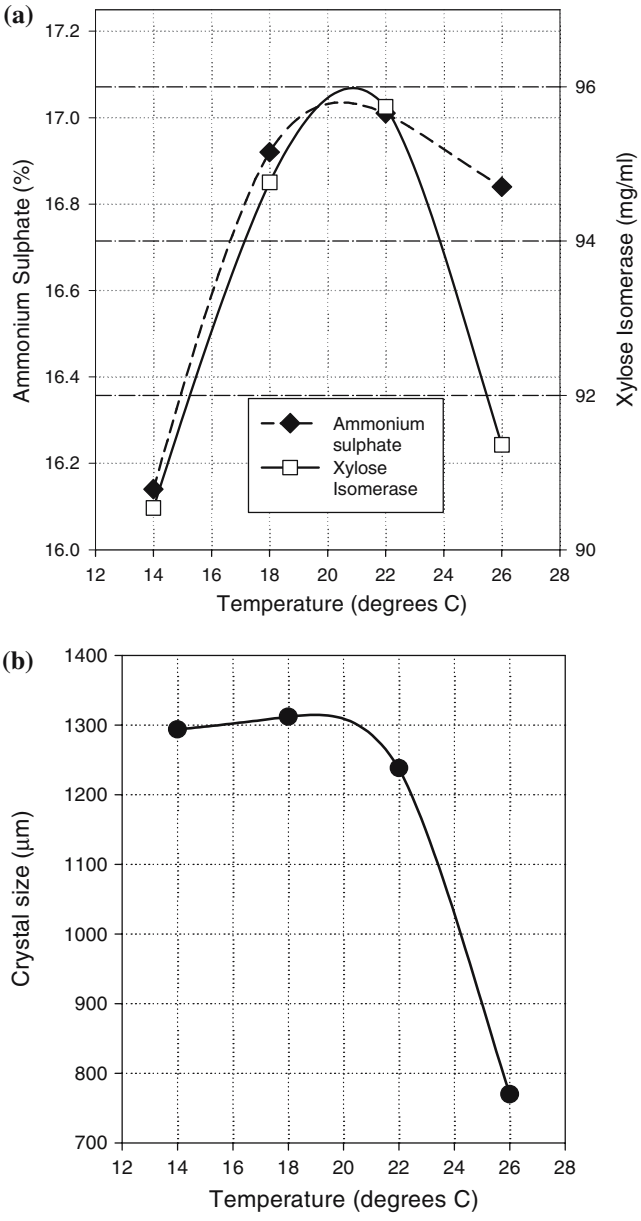

Fig. 9 Graph showing **a** the optimum precipitant conditions for a given temperature to grow the largest crystals and **b** the crystal size as a function of temperature

Discussion and conclusions

In the system studied the experimental design and response surface mapping aided the optimization of crystal volume. In the statistically best case, eightfold replicates of conditions, the model derived from response surface mapping explained 66% of the experimental data. The accuracy of the model decreased with the number of replicates. A critical factor in the success of the technique was the reproducibility of crystallization conditions. In our case we made use of the technique specifically to enable neutron diffraction studies of the xylose isomerase enzyme mechanism. Establishing its power as a general technique will require studies on significantly more macromolecules. Interestingly knowledge of protein solubility, a time consuming step requiring large amounts of sample (Darcy and Wiencek 1998; Nakazato et al. 2004; Rosenberger et al. 1993), was not required for the optimization. Simply knowing the initial crystallization condition producing crystals suitable for X-ray analysis and the associated optimization range was sufficient to apply the techniques in this case. The response surface determined with very little material led to a model describing the results. This enabled scaling up of the crystallization volume to achieve the largest crystals, Fig. 7(ii). It should be noted that while the model predicts the experimental results it is not necessarily a robust mathematical description of the crystallization process.

Simply changing the solvent from H_2O to D_2O significantly affected our results, more so than might have been anticipated from an effect of pH alone. In D_2O solutions we obtained many small crystals in the form of needles when we used conditions optimized with H_2O solutions. In H_2O solutions, similar needles had been observed at ammonium sulfate and protein concentrations significantly above the optimum conditions for which large single crystals formed. Assuming a similar trend in the D_2O system, a reduction of the ammonium sulfate and protein concentration produced large crystals in D_2O. With current knowledge it is not possible to directly translate optimal crystal growth conditions in H_2O to optimal conditions in D_2O. However, conditions in H_2O were adequate to enable neutron diffraction.

Experimental design and response surface methods can easily be used with any number of variables although this affects the number of experiments and the ease of graphically interpreting the results. We chose to look at temperature as an additional variable but kept the interpretation simple by studying it as a separate variable rather than integrated into a full three-dimensional design. Temperature as a crystallization variable has been investigated in a number of studies (Christopher et al. 1998; Judge et al. 1999; Long et al. 1994; Rosenberger et al. 1993). In our case there was a considerable change in optimum crystallization conditions as a function of temperature. The crystal size is rapidly reduced when crystallization takes place at temperatures approaching the upper end of the temperature range studied. For our experimental neutron data collection, described elsewhere (Meilleur et al. 2006), crystals were transported to the Institute Laue

Table 3 Summary of the total number of experiments (repeated at each temperature) and the breakdown of those experiments with the analysis of the model to the experimental data

Experiment					
Total number of experiments	72	36	26	26	18
Replicates of factorial points	8	4	2	4	2
Replicates of axial points	8	4	4	2	2
Replicates of center point	8	4	2	2	2
Results					
Model significance (F value)	40.67	17.18	14.00	13.79	5.84
Lack of fit (F value)	17.27	12.78	8.48	8.85	4.64
Prediction power	23.38	15.27	14.32	13.37	8.66
Adjusted R^2	0.659	0.613	0.621	0.617	0.488
Predicted R^2	0.639	0.563	0.539	0.539	0.336

Table 4 Predicted crystal size in microns as a function of pH, and H_2O or D_2O growth

	pH 7.3			pH 7.7			pH 8.1		
	XI (mg/ml)	$AmSO_4$ (%)	Size	XI (mg/ml)	$AmSO_4$	Size	XI (mg/ml)	$AmSO_4$ (%)	Size
H_2O	–	–	–	67.3	18.0	5,779	60.5	16.6	998
	pD 7.7			pD 8.1					
	XI (mg/ml)	$AmSO_4$ (%)	Size	XI (mg/ml)	$AmSO_4$	Size			
D_2O	59.1	16.4	889	80.0	18.0	1,402	–	–	–

Langevin in Grenoble, France from Huntsville, AL, USA. The crystals were sealed in capillaries also containing mother liquor. Because we had no temperature control during transportation the conditions that produced the largest crystals at 22°C rather than those which produced the largest crystals overall, at 18°C, were used. This most closely matched the ambient temperature during the transport and reduced the possibility of crystal degradation. During crystal volume optimization temperature is clearly an important variable and based on our data from this study we conclude that at a minimum crystal size optimization should be performed at two temperatures to determine if this variable has a significant effect on final crystal size.

We have optimized crystal size, i.e. maximized the dimensions visible in observations of the crystals in one direction of view. This optimization worked well in our case. For crystals that have plate morphology optimization of length and width will not necessarily lead to an improvement in depth, which is critical for increasing diffraction volume. This is a limitation of the technique and overcoming it would necessitate the visualization of the crystals in three dimensions. The use of crystal size (or volume) as a metric in any crystallization technique immediately opens the technique to automation. Unlike image analysis for identifying growing crystals from precipitant, phase separation and other conditions, we have a clearly defined metric. Image analysis methods to measure object sizes are mature and reasonably robust. Robotic technology for liquid dispensing coupled with experimental design, response surface mapping and automated image analysis can conceivably provide a platform for volume optimization of many samples simultaneously.

The principle limitation in utilizing neutron diffraction for structural studies has been signal-to-noise ratio in the diffraction data. With the simultaneous construction of new, more intense neutron sources, the development of dedicated beamlines and detectors, perdeuteration techniques and simple volume optimization methods such as the one here reported, the number of questions amenable to neutron diffraction study will grow and neutron diffraction as a technique will rapidly grow in scientific use over the next decade.

Acknowledgments We would like to thank Genencor International for the generous donation of the xylose isomerase used in this study, Riccardo Leardi for initial discussions on experiment design and Richard Kephart for assistance in the initial stages. MvdW and MD are contractors to NASA through BAE Systems Analytical Solutions. This work was supported through NASA grant NAG8-1916 and the Oishei Foundation.

References

Asboth B, Naray-Szabo G (2000) Mechanism of action of D-xylose isomerase. Curr Protein Pept Sci 1:237–254

Broutin I, Ries-Kautt M, Ducruix A (1995) Lysozyme solubility in H_2O and D_2O solutions as a function of sodium chloride concentration. J Appl Cryst 28:614–617

Budayova-Spano M, Lafont S, Astier JP, Ebel C, Veesler S (2000) Comparison of solubility and interactions of aprotinin (BPTI) solutions in H_2O and D_2O. J Cryst Growth 217:311–319

Burke MW, Leardi R, Judge RA, Pusey ML (2001) Quantifying main trends in lysozyme nucleation: the effect of precipitant concentration, supersaturation and impurities. Cryst Growth Design 1:333–337

Carrell HL, Glusker JP, Burger V, Manfre F, Tritsch D, Biellmann JF (1989) X-ray analysis of D-xylose isomerase at 1.9 A: native enzyme in complex with substrate and with a mechanism-designed inactivator. Proc Natl Acad Sci USA 86:4440–4444

Carter CC (1994) Quantitative analysis in the characterization and optimization of protein crystal growth. Acta Crystallogr D Biol Crystallogr 50:572–590

Carter CW Jr, Carter CW (1979) Protein crystallization using incomplete factorial experiments. J Biol Chem 254:12219–12223

Chayen NE (1998) Comparative studies of protein crystallization by vapour-diffusion and microbatch techniques. Acta Crystallogr D Biol Crystallogr 54(Pt 1):8–15

Christopher GK, Phipps AG, Gray RJ (1998) Temperature-dependent solubility of selected proteins. J Cryst Growth 191:820–826

Darcy PA, Wiencek JM (1998) Estimating lysozyme crystallization growth rates and solubility from isothermal microcalorimetry. Acta Crystallogr D Biol Crystallogr 54:1387–1394

Farber GK, Glasfeld A, Tiraby G, Ringe D, Petsko GA (1989) Crystallographic studies of the mechanism of xylose isomerase. Biochemistry 28:7289–7297

Fenn TD, Ringe D, Petsko GA (2004) Xylose isomerase in substrate and inhibitor michaelis states: atomic resolution studies of a metal-mediated hydride shift. Biochemistry 43:6464–6474

Glasoe PK, Long FA (1960) Use of glass electrodes to measure acidities in deuterium oxide. J Phys Chem 64:188–189

Gripon G, Legrand L, Rosenman I, Vidal M, Robert MC, Boue F (1997a) Lysozyme–lysozyme interactions in under- and super-saturated solutions: a simple relation between the second virial coeffieicnts in H_2O and D_2O. J Cryst Growth 178:575–584

Gripon G, Legrand L, Rosenman I, Vidal O, Robert MC, Boue F (1997b) Lysozyme solubility in H_2O and D_2O solutions: a simple relationship. J Cryst Growth 177:238–247

Hazemann I, Dauvergne MT, Blakeley MP, Meilleur F, Haertlein M, Van Dorsselaer A, Mitschler A, Myles DA, Podjarny A (2005) High-resolution neutron protein crystallography with radically small crystal volumes: application of perdeuteration to human aldose reductase. Acta Crystallogr D Biol Crystallogr 61:1413–1417

Judge RA, Jacobs RS, Frazier T, Snell EH, Pusey ML (1999) The effect of temperature and solution pH on the nucleation of tetragonal lysozyme crystals. Biophys J 77:1585–1593

Liu XQ, Sano Y (1998a) Effect of Na+ and K+ ions on the initial crystallization process of lysozyme in the presence of D_2O and H_2O. J Protein Chem 17:479–484

Liu XQ, Sano Y (1998b) Kinetic studies on the initial crystallization process of lysozyme in the presence of D_2O and H_2O. J Protein Chem 17:9–14

Long MM, DeLucas LJ, Smith C, Carson M, Moore K, Harrington MD, Pillion DJ, Bishop SP, Rosenblum WM, Naumann RJ, Chait A, Prahl J, Bugg CE (1994) Protein crystal growth in microgravity-temperature induced large scale crystallization of insulin. Microgravity Sci Technol 7:196–202

Meilleur F, Dauvergne MT, Schlichting I, Myles DA (2005) Production and X-ray crystallographic analysis of fully deuterated cytochrome P450cam. Acta Crystallogr D Biol Crystallogr 61:539–544

Meilleur F, Snell EH, van der Woerd MJ, Judge RA, Myles DA (2006) A Quasi-Laue neutron crystallographic study of D-xylose isomerase. Eur Biophys J (in press)

Nakazato K, Homma T, Tomo T (2004) Rapid solubility measurement of protein crystals as a function of precipitant concentration with micro-dialysis cell and two-beam interferometer. J Synchrotron Radiat 11:34–37

Niimura N (1999) Neutrons expand the field of structural biology. Curr Opin Struct Biol 9:602–608

Rosenberger F, Howard SB, Sowers JW, Nyce TA (1993) Temperature-dependance of protein solubility—determination and application to crystallization in X-ray capillaries. J Cryst Growth 129:1–12

Shu F, Ramakrishnan V, Schoenborn BP (2000) Enhanced visibility of hydrogen atoms by neutron crystallography on fully deuterated myoglobin. Proc Natl Acad Sci USA 97:3872–3877